USE OF STEEL FIBER REINFORCED CONCRETE FOR BLAST RESISTANT DESIGN

by

DEIDRA KALMAN

B.S., Kansas State University, 2010

A REPORT

Submitted in partial fulfillment of the

requirements for the degree

MASTER OF SCIENCE

Department of Architectural Engineering and Construction Science
College of Engineering

KANSAS STATE UNIVERSITY
Manhattan, Kansas

2010

Approved by:
Major Professor
Kimberly Waggle Kramer, P.E.

Abstract

Reinforced concrete is a common building material used for blast resistant design. Adding fibers to reinforced concrete enhances the durability and *ductility* of concrete. This report examines how adding steel fibers to reinforced concrete for blast resistant design is advantageous.

An overview of the behavior of blasts and goals of blast resistant design, and advantages of reinforced concrete in blast-resistant design, which include mass and the flexibility in detailing, are included in the blast resistant design section. The common uses for fiber-reinforced concrete, fiber types, and properties of fiber reinforced concrete varying with fiber type and length, and concrete strength are discussed in the fiber-reinforced concrete section. Two studies, *Very High-Strength Concrete for Use in Blast-and-Penetration Resistant Structures* and *Blast Testing of Ultra-High Performance Fiber and FRP-Retrofitted Concrete Slabs*, are reviewed. Lastly, the cost, mixing and corrosion limitations of using steel fiber-reinforced concrete are discussed.

Reinforced concrete has been shown to be a desirable material choice for blast resistant design. The first step to designing a blast resistant reinforced concrete structure is to implement proper detailing to ensure that structural failures will be contained in a way that preserves as many lives as possible. To design for the preservation of lives, a list of priorities must be met. Preventing the building from collapse is the first of these priorities. Adding steel fibers to concrete has been shown to enhance the concrete's post-crack behavior, which correlates to this priority. The second priority is reducing flying debris from a blast. Studies have shown that the failure mechanisms of steel fiber reinforced concrete aid in reducing flying debris when compared to conventional reinforced concrete exposed to blast loading.

The major design considerations in designing steel fiber reinforced concrete for blast resistant design include: the strength level of the concrete with fiber addition, fiber volume, and fiber shape. As research on this topic progresses, the understanding of these factors and how they affect the strength characteristics of the concrete will increase, and acceptance into the structural design industry through model building codes may be possible.

Table of Contents

List of Figures

List of Tables

Acknowledgments

I would like to take this opportunity to sincerely thank my committee for their time and thoughtful feedback on this report. Specifically, I would like to recognize Kimberly Kramer for her guidance throughout the process of reading, writing, and presenting.

1.0 Introduction

When explosion is a design criterion for buildings either due to the combustible materials contained within the structure or due to an intentional explosion (bomb), a common material chosen for blast resistance design is reinforced concrete, because of its large mass and flexibility in detailing. The use of fibers in concrete is a common design practice for the reduction of cracks in concrete slabs, among other benefits. The possibility of fiber reinforced concrete satisfying blast resistant design requirements for external blasts more effectively than conventionally reinforced concrete is examined in this study. It also addresses goals and techniques for blast resistant design, introduces fiber reinforced concrete applications, and fiber types, and determines properties of steel fiber reinforced concrete through impact loading tests. Additionally, this report examines previous research by others that tested steel fiber reinforced concrete under blast loading, and explores limitations of steel fiber reinforced concrete.

Accordingly, Section 2 introduces the behavior of blast loading on a structure. This is fundamental to understanding the expectations of a member designed to be blast resistant. Next, follows a brief discussion of the expectations of blast resistant design, as defined by the U.S. Army Corp of Engineers, and how to detail reinforced concrete members to meet expectations. The final discussion in the Blast Resistant Design Section is the advantages of using reinforced concrete in blast resistant design, and, to substantiate the argument for using Fiber Reinforced Concrete for blast resistant design.

A general overview of Fiber-Reinforced Concrete (FRC) is presented in Section 3. Current uses of FRC are presented to examine the properties accepted by engineers in the design field. An overview of fiber types, including available materials and shapes, gives background for studies in further reading. In particular, the report covers flexural and shear behavior of FRC under impact loading via several studies, a few of which are presented in Section 4 to demonstrate FRC's benefits as a blast resistant material.

To build upon the findings of the impact loading studies, two studies examine different concrete strengths and fiber properties under blast loading.

Finally, discussion of limitations of FRC, cost, mixing and placing, and corrosion potential, covered in Section 5, complete the perspective on what an engineer would need to consider to adopt FRC as a blast resistant design material.

2.0 Blast Resistant Design

The United States military has been testing and designing structures for blast resistance for several decades. Over the past decade, the private sector has been developing standards for blast resistance design, using the military's parameters for guidance. Through testing done by the U.S. Army Corps of Engineers and private associations, engineers and researchers have studied the behavior of blasts so that structural members can be adequately designed for blast events. Since blast loading is an extreme loading event, reasonable assumptions (such as large deformations and strategic failures) are required to maintain an economical design (Agnew, Marjanishvili, & Gallant, 2007). Reinforced concrete is one material that can meet the demands of blast resistant design because of its large mass and flexibility in detailing (Galinat, 2007).

2.1 Behavior of Blasts

"An explosion is a rapid release of energy taking the form of light, heat, sound and a shock-wave. The shock wave consists of highly compressed air that wave-reflects off the ground surface to produce a hemispherical propagation of the wave that travels outward from the source at supersonic velocities" (Hinman, 2003). The shockwave of a blast can reflect off a surface with an amplification factor up to 13, compared to an accoustical wave, which can reflect with an amplification factor up to two. The amplification factor is influenced by the distance the schockwave travels before reflection and by the angle of incidence.

This event differs from other loading types for buildings because of its short duration and high pressures. The time interval for the blast wave, t_d, is between 0.1 and 0.001 seconds; the natural period of the structure, T_n, ranges from 0 to 8 seconds, depending on building height, framing system, and loading scenario (Jacobs, 2008). "For situations where $t_d<0.4T_n$ (some sources advise $t_d<0.1T_n$), the blast wave effectively imparts an initial velocity to a structural element, and the element then continues to respond at its natural frequency" (McCann & Smith, 2007). Moreover, the initial velocity (load being applied to the structure) is determined by the blast wave duration, force, and mass of the structure. "This load response to a blast is significantly different from the load response to a seismic event, for which the natural frequency

of the structure, rather than the mass, is the primary factor in the response" (McCann & Smith, 2007).

Another consideration in designing structural members for blast resistant design is load reversals. Late into the shockwave's phase, the pressure becomes negative, creating a suction force. A graph of this response, where the blue dotted line indicates initial wave pressures and the red solid line indicates reflected wave pressures, is shown below in Figure 2.1-1. Clearly, the reflected pressures are stronger than the initial pressures, as mentioned previously. Immediately following the suction force, surfaces experience a drag pressure as air rushes in bringing flying debris. "In an external explosion, a portion of the energy is also imparted to the ground, creating a crater and generating a ground shock wave analogous to a high-intensity, short-duration earthquake" (Hinman, 2003).

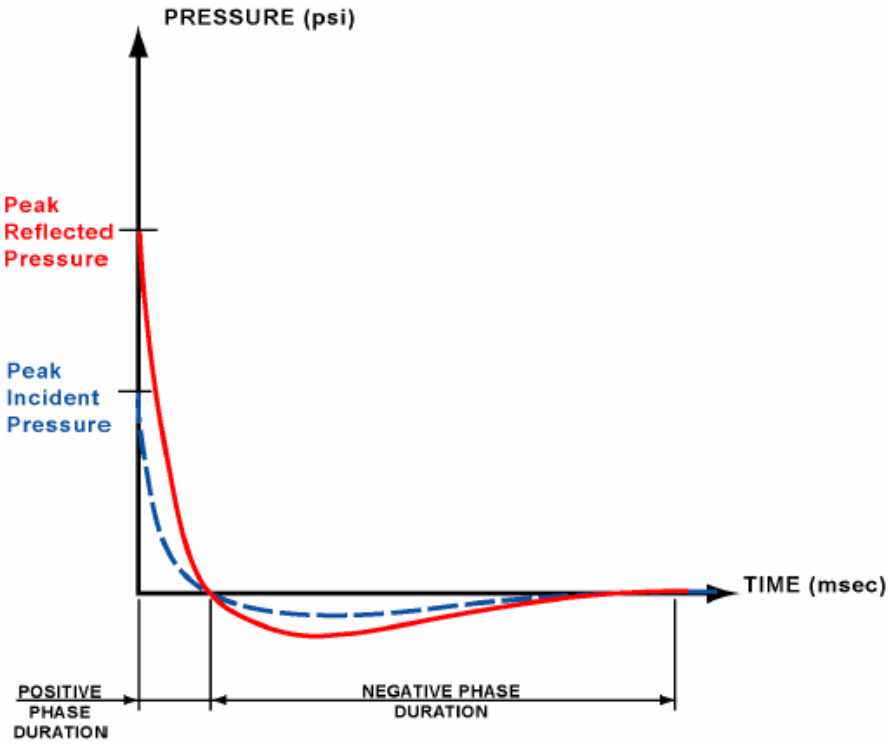

Figure 2.1-1 Air-blast pressure response over time (Hinman, 2003)

The extent of damage caused by a blast is determined by two factors: (1) explosive size measured in pounds of TNT and (2) distance between explosive and affected structural member.

Figure 2.1-2, for example, illustrates the pressure differences between two different sizes of explosives at varying distances, where it is apparent that range and incident pressure have a non linear relationship, and that explosive weight has less influence on incident pressure as the range increases. Furthermore, two threats are considered in blast resistant design and the size of the explosive is related to the threat type. These two threats are vehicle weapons and hand-delivered weapons. Hand-delivered weapons typically range from 2.3 kg (5 lbs.) to 45.4 kg (100 lbs.) of TNT. Meanwhile, vehicle weapons, by far the larger threat, are typically greater than one hundred pounds of TNT. Vehicle weapons pose the greater threat to the structure due to their size and potential site of detonation, an example of this type of threat would be the bombing of the Alfred P. Murrah Federal Building in Oklahoma City, Oklahoma in April of 1995; however their rate of occurrence is far less than that of hand delivered weapons. "To put the weapon size into perspective, it should be noted that thousands of deliberate explosions occur every year within the United States, but the vast majority of them have weapon yields less than 2.3 kg (5 lbs.). The number of large-scale vehicle weapon attacks that have used hundreds of pounds of TNT during the past twenty years is by comparison very small" (Hinman, 2003). Ultimately, the owner and the security and protective design consultants work together to determine the size of weapon to design for (Hinman, 2003).

Another consideration is the distance the structural member is from the explosion, which affects the magnitude of the load. When a blast occurs relatively close to the structural element, it may shatter the concrete in the immediate vicinity, a phenomenon referred to as breach (Agnew, Marjanishvili, & Gallant, 2007). A similar behavior is exhibited by the impact of a bullet or explosion shrapnel (Millard, Molyneaux, Barnett, & Gao, 2010). Specifically, direct shear governs when the distance between the structural element and the explosion site increases, and a relatively small area experiences high air blast pressures. Finally as the distance grows between the structural element and explosion, the pressures are distributed over a greater area so that flexure is the governing response. Section 3.0 *Fiber Reinforced Concrete* covers correlation of these loadings with fiber reinforced concrete testing.

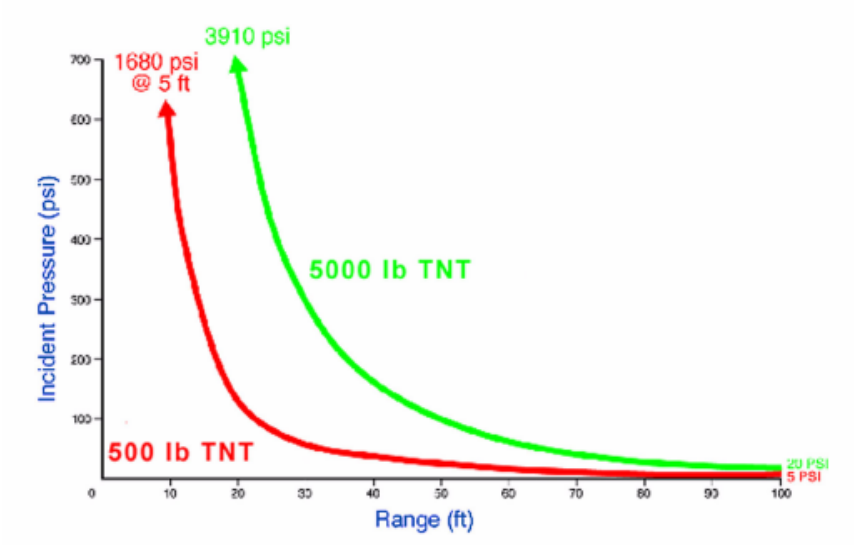

Figure 2.1-2 Incident pressures of different explosive charge weights (Hinman, 2003)

2.2 Goals of Blast Resistant Design

"Blast-resistant design is element-focused. It enhances *toughness*, *ductility*, strength and dynamic characteristics of individual structural elements for resistance to air-blast induced loading" (McCann & Smith, 2007).

In particular, the goals of blast resistant design are relatively modest compared to most other load scenarios with the exception of seismic. Gravity loads are predicted by codes, and structural engineers design structural elements to withstand these loads, without yielding or permanent deformation of the structural elements. Thus, when designing a structure to resist wind loads, every element of the structure is designed to sustain an expected pressure. Quite simply, the failure of a structural component due to wind loading, excluding tornadic events, is unacceptable in design practice. Seismic design is most closely related to blast resistant design in that predetermined structural elements are designed to yield and buckle during the seismic event to ensure that progressive collapse does not occur. Also, similarly to seismic design, blast design accounts for the occupancy of the building to determine the level of protection required.

However, blast loading differs from any other loading event in a few significant ways. First, the magnitude of the pressures acting on the building during a blast event can be many orders of magnitude greater than those of pressures experienced in any other loading. "It is not

uncommon for the peak pressure on the building from a vehicle weapon parked along the curb to be in excess of 690 kPa (100 psi)" (Hinman, 2003). Therefore, failure of building components is expected. Secondly, a wide variety of pressures are imposed on the building, since blast pressures decay rapidly with distance. Accordingly, many types of damage will occur and it will be more localized, compared to that of other hazards. Lastly, duration of the event is measured in milliseconds, rather than seconds. (Hinman, 2003)

Notably, it would not be economical to design every building for a high level of protection, where "no visible permanent damage" is experienced (McCann & Smith, 2007). Therefore, the primary goal is to save lives, not the building, and so the following is a prioritized list of goals:

1) preventing the building from collapse
2) reducing flying debris
3) facilitating evacuation and rescue/recovery efforts. (Agnew, Marjanishvili, & Gallant, 2007)

First, preventing building collapse means the columns and floor slabs must be given particular consideration in design, since their failure could initiate a progressive collapse. Floor slabs are particularly vulnerable to vehicle-delivered explosions because of their large surface area for the explosive pressures to act on and their relatively small thickness. The consequence of losing the floor slab is the increased unbraced length of the column, which could cause the column to buckle. As illustrated in Figure 2.2-1, the structure's floor and column elements are the most susceptible to the blast loading, due to the sequence of the blast wave.

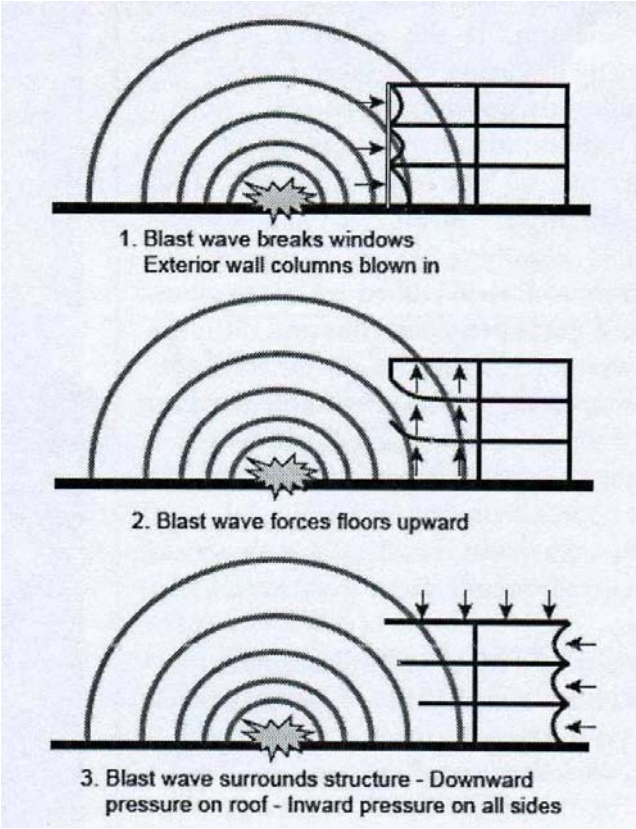

Figure 2.2-1 Succession of blast pressure waves on a building (Agnew, Marjanishvili, & Gallant, 2007)

The *ductility* of columns is an important design consideration to ensure proper energy absorption. The "ductile detailing of primary members and connections allows for large deformations while maintaining load-carrying capacity" (Agnew, Marjanishvili, & Gallant, 2007). This *ductility* can be accomplished through proper detailing, which is discussed in the *Flexibility in Detailing* section. Additionally, Section 3.0 *Fiber Reinforced Concrete* addresses *ductility* due to fibers.

Although reducing flying debris caused by the impact of the explosion on windows and walls is the second priority, it can be a major source of injuries and fatalities. When the blast wave encounters a concrete member, failure in tension of the material in the cover zone, which is the area of concrete covering the tensile reinforcement, occurs because concrete has a small tensile

capacity (Millard, Molyneaux, Barnett, & Gao, 2010). Fortunately, this area of blast resistant design offers the greatest potential for adding fiber to reinforced concrete.

The structural engineer has the least control over the third priority of facilitating evacuation and rescue/recovery efforts. Nevertheless, "Evacuation, rescue and recovery efforts can be significantly improved through effective placement, structural design, and redundancy of emergency exits and critical mechanical/electrical systems" (Agnew, Marjanishvili, & Gallant, 2007). This priority is not a major consideration for this report, while the first two priorities are.

2.3 Advantages of Reinforced Concrete in Blast Resistant Design

Reinforced concrete is the most common material for blast resistant design, due to its availability, relatively low cost, mass, and flexibility of detailing. (Lane, Craig, & Babcock, 2002) However, to understand the advantages of adding fiber to reinforced concrete, structural engineers first need to understand the advantages of using reinforced concrete even without fibers.

2.3.1 Mass

Reinforced concrete "ranks second to steel as a stand-alone material in its ability to withstand blast overpressures, mostly due to its mass" (Lane, Craig, & Babcock, 2002). The initial velocity a structure experiences during a blast is inversely proportional to its mass. Therefore, a dense material such as concrete has an advantage in resisting blast loads (McCann & Smith, 2007). Figure 2.3.1-1 illustrates the effect of mass on the resistance of a structure to blast forces. Clearly, the more massive 25.4 cm (10") wall shows a higher resistance, or less excitation, to the blast load and a shorter period as compared to the 20.3 cm (8") wall. Both walls respond to the blast load with decreasing amplitude, due to the 2% damping used in this trial.

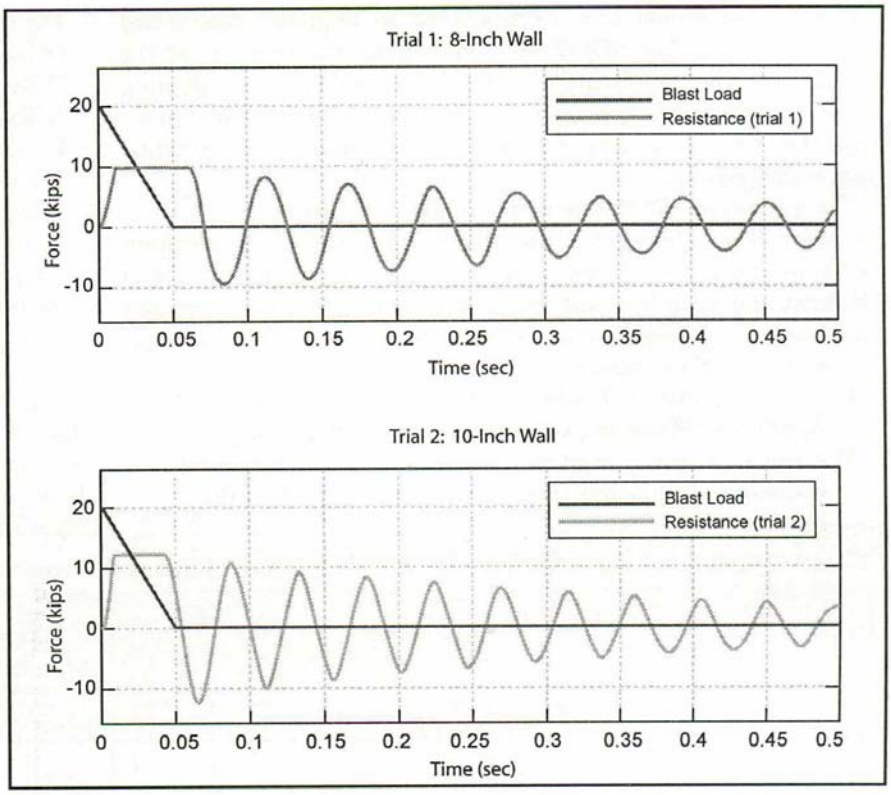

Figure 2.3.1-1 Applied force and internal resistance time histories (using 2% damping) (McCann & Smith, 2007)

2.3.2 Flexibility in Detailing

The *compressive strength* of concrete is approximately ten times greater than its tensile strength and therefore steel reinforcing bars are added in the tension region of the elements to be an effective structural member. Naturally, in blast design, the structural engineer assumes that the structural elements will be loaded beyond their yield strength and up to failure. Also, as illustrated in Figure 2.2-1(2), members need to be designed for load reversals, particularly slabs and columns which could experience loading in the opposite direction of gravity loading. To account for this, reinforcing steel must be placed in both the top and bottom of slabs to meet tensile capacity expectations, and also, splices in columns should be design for tension. Therefore, detailing of reinforced concrete elements is critical to achieve ductile structural behavior to resist blast loading. Some general guidelines for detailing follow:

- "Limit concrete *compressive strength*s to 34,480 kPa (5,000 psi) or less, since elements with higher strength concrete will experience more brittle modes of failure when subjected to inelastic yielding."
- "Design for load reversals, which can subject elements to loads for which they were not designed; for example, tension in a column due to floor slab uplift", as shown previously in Figure 2.2-1.
- "Ensure that the ratio of the steel reinforcement's actual tensile strength to actual yield strength is not less than 1.25 for sufficient yield capability."
- "Locate lap splices outside of the hinge region of an element as predicated by the design air blast threat."
- "Design lap splices as tension splices. With [a] blast, localized loading locations are unpredictable and hinge regions could be located anywhere along the length of the member" (Agnew, Marjanishvili, & Gallant, 2007).

These are general guidelines, intended to give the reader an idea of the considerations for blast resistant design. Meanwhile, later sections will cover the impact of adding fiber to reinforced concrete and how it could benefit blast resistant design.

3.0 Fiber-Reinforced Concrete

The Portland Cement Association (PCA) has been investigating adding fiber to reinforced concrete since the late 1950's, and several studies have investigated the behavior of fiber reinforced concrete (FRC) under impact loading. Moreover, fiber is currently used in applications that require enhanced crack control and/or better performance in flexure and shear (ACI Committee 544, 1996). Several fiber types are available depending on the application and desired behavior. This report addresses selective studies to provide evidence supporting the use of fibers in reinforced concrete for blast resistant design.

3.1 Common Uses for Fiber-Reinforced Concrete

"FRC has been used successfully in structures subjected to bending and/or shear such as highway bridge slabs, piles, tunnel linings, architectural concrete, precast elements, offshore structures, structures in seismic regions, thin and thick repair, crash barriers, footings, and various hydraulic structures. FRC exhibits better performance not only under static and quasi-statically applied loads but also under fatigue, impact, and impulse loadings and under environmentally imposed cracking" (Higashiyama & Banthia, 2008). Additional elements that may include fibers in reinforced concrete are industrial flooring, which can be exposed to abrasive loading, and air-field pavements (Suaris & Shah, 1983). Both loading situations require the concrete to have a high energy absorption rate and *toughness*.

3.2 Fiber Types

Many different fiber types are available: steel, micro-synthetic, macro-synthetic, glass, cellulose, natural, and poly-vinyl alcohol (PVA) fibers. These types have varying properties and applications. Fibers to control plastic shrinkage cracking are micro-synthetic fibers, which are made of synthetic materials such as polypropylene, nylon, polyethylene, and polyester. Macro-synthetic fibers have properties similar to steel fibers and can be used in their place (Applications , 2007). The first glass fibers produced were attacked by the alkai in the cement and destroyed; therefore, they are manufactured today with zirconia, and their most common application is in "exterior architectural cladding panels" (ACI Committee 544, 1996). Steel fibers are used to enhance the "*toughness* and post-crack load carrying capacity," and their lengths vary from 38.1

mm (1.5”) to 76.2 mm (3”). “Typically loose or bundled, these fibers are generally made from carbon or stainless steel and are shaped into varying geometries such as crimped, hooked end or with other mechanical deformations for anchorage in the concrete” (Applications , 2007). Steel fibers are the material investigated for their mechanical properties in this study.

A variety of steel fiber shapes are available: straight, crimped, hooked single, hooked collated, and twisted (Tadepalli, Mo, Hsu, & Vogel, 2009). Before the mid-1970’s, the only fiber shape tested was straight. Currently, straight fibers are seldom used in the field, due to their inferior mechanical bond to concrete compared to that of deformed fibers. The most effective shape for energy absorption capacity is hooked fibers according to studies on effects of steel fiber reinforcement on the mechanical properties of reinforced concrete (Tadepalli, Mo, Hsu, & Vogel, 2009).

3.3 Properties of Fiber Reinforced Concrete

Steel fiber reinforced concrete has undergone much testing to determine its mechanical properties, and is described in ACI document ACI 544.1 R-96 *Fiber Reinforced Concrete* as “a concrete with increased *strain* capacity, impact resistance, energy absorption, fatigue endurance, and tensile strength” (ACI Committee 544, 1996). This information is vital to integrating steel fibers into reinforced concrete design properly. Accordingly, the following sections present several studies published by the American Society of Civil Engineers (ASCE) and the American Concrete Institute (ACI).

3.3.1 Effect of Different Fiber Types, Lengths, and Concrete Strengths on Mechanical Properties

The first study is *Mechanical Properties of Steel Fiber Reinforced Concrete Beams* by Padmanabha Tadepalli, Y.L. Mo, Thomas Hsu, and John Vogel. This study explores the mechanical properties (*compressive strength*, first-crack flexural strength, and ultimate flexural strength, *modulus of elasticity*, flexural *toughness*, and *ductility*) of fiber reinforced concrete beams based on fiber content, fiber length, and type.

Two concrete mixes were tested; one traditional concrete with aggregates, cement, and water, and another mix with fly ash added and less water content to attain increased strength. “The

steel fibers used were hooked-collated long (Dramix), hooked-collated-short (Dramix), hooked single (Royal) and twisted (Helix)" (Tadepalli, Mo, Hsu, & Vogel, 2009). Two different Dramix fibers, long and short, were tested with lengths of 2.4" and 1.2" respectively, Royal fibers had a length of 1.6" and finally the Helix fibers had a length of 1.0". Another significant property, aspect ratio, is found by dividing the length by the diameter of the fiber. The properties of these fibers are given below:

Table 3.3.1-1 Properties of fibers used in testing (Tadepalli, Mo, Hsu, & Vogel, 2009)

Fiber		Length (inch)	Diameter (inch)	Aspect Ratio
Dramix	Long Fiber	2.4	0.03	80
	Short Fiber	1.2	0.022	55
Royal		1.6	0.03	53
Helix		1.0	0.02	50

All four fiber types were added to the higher strength concrete mix, and only the Dramix (long and short) fibers were added to the traditional concrete. Among these mixes, two different fiber volume fractions were used: 0.5% and 1.5% by volume.

The test was performed on beams with cross sectional dimensions of 152 mm x 152 mm x 508 mm (6" x 6" x 20"). Three specimens tested for each mix were subjected to a two-point loading flexural test, following the guidelines of ASTM C 1609.

Testing of the specimens showed that concrete with steel fibers had increased *ductility* when compared to concrete beams with no steel fibers. Specifically, the failure mode of the concrete containing steel fibers was different from the failure of the concrete with no fibers. Instead of a sudden brittle failure as is typical of concrete with no steel fiber reinforcing, the steel fiber reinforced concrete developed initial cracks, but then sustained additional load as the steel fibers prevented cracks from spreading; "randomly oriented fibers crossing the crack resisted the propagation of cracks and separation of the section" (Tadepalli, Mo, Hsu, & Vogel, 2009). Eventually, the failure of the fiber and concrete bond led to the beam failure. The ultimate load

capacity of the steel fiber reinforced concrete depended on several steel fiber characteristics: fiber content, fiber tensile strength, fiber shape and fiber bond strength.

The hooked collated long fibers withstood the highest loading, followed by twisted fibers at a fiber content of 0.5% by volume. For the fiber content of 1.5% by volume the hooked collated short fibers had the maximum load capacity. The authors noted that the hooked collated long fibers and twisted fibers had poor workability with a fiber content of 1.5% by volume. The results showed that the higher fiber content yielded increased ultimate load capacity for all the mixes as long as the mixes were workable. Also, the advantage of long fibers over short fibers was apparent at fiber content of 0.5%, but less advantageous at 1.5% fiber content. These results are consistent in both normal and *high strength concrete*. Overall, hooked collated fibers showed the best flexural strength, regardless of the strength of concrete used. Researchers also observed that fiber type and length was more important at low concrete strengths and less significant at higher strengths.

This study concludes that flexural capacity increased from 30% to 120% when the fiber content increased from 0.5% to 1.5%. The study also concluded that the length of fibers was a significant factor in hooked shaped fibers at low percentages, but as the fiber percentage increased, the significance of fiber length diminished. Overall, the hooked collated and twisted fibers performed the best; however, the poor workability of the twisted fibers means that the hooked collated fibers are preferable.

3.3.2 Effect of Different Concrete Strengths

Another technical paper, *Mechanical Properties of Steel Fiber-Reinforced Concrete*, published by the Journal of Materials in Civil Engineering investigated the strength properties of FRC by testing three grades of concrete: normal strength concrete (35 MPa [5,076 psi]), moderately high-strength concrete (65 MPa [9,428 psi]), and high-strength concrete (85 MPa [12,328 psi]). Silica fume was added to the 85 MPa (12,328 psi) concrete mix, and a superplasticizer was added to both the 65 MPa (9,428 psi) and 85 MPa (12,328 psi) concrete mixes. Also, hooked-end fibers were added at a fiber dosage between 0.0 and 1.5% test specimens consisting of cubes and cylinders. Then, "The cube and cylinder specimens were tested to determine the *compressive strength* according to IS: 516 (BIS 1959), while cylinder specimens were tested for *split tensile strength* according to IS: 5816 (BIS 1999). Also, a

modulus of rupture test was carried out according to IS: 516 (BIS 1959). Finally, *modulus of elasticity* and *Poisson's ratio* were determined using the standard cylinder specimens (BIS 1959)" (Thomas & Ramaswamy, 2007).

This research resulted in several findings of interests; one was that "the average increase in cube *compressive strength* due to the addition of steel fibers was found to be minimal", but the biggest increase in cube *compressive strength* occurred in the normal strength concrete test specimens (Thomas & Ramaswamy, 2007). Tests for cylinder *compressive strength* showed that normal-strength concrete had the greatest strength increase at 8.33% with the addition of fibers, but that still was judged to be a minimal increase. However, *split tensile strength* tests with fibers showed an increase of 38.2% in normal-strength concrete, 41.2% in moderately high-strength concrete, and 38.5% in high-strength concrete. Similar increases of 46.2% in normal-strength concrete, 38.8% in moderately high-strength concrete, and 40.0% in high-strength concrete were observed for *modulus of rupture* tests with fibers. Researchers discovered the fibers bridged the cracks that develop in the concrete matrix and determined this was the mechanism that enhances the tensile strength characteristics (Thomas & Ramaswamy, 2007).

Meanwhile, adding fibers had little effect on *Poisson's ratio* since the key factor is the behavior during initial loading and the fibers don't provide a significant advantage at this stage. Another property that benefited minimally from adding fibers was the *modulus of elasticity* because it is measured from the linear portion of the *stress-strain* relationship, where the effect of the fibers is insignificant (Thomas & Ramaswamy, 2007).

An area that showed considerable improvement was the *strain* corresponding to the peak compressive *stress*. An increase of 29.5% was shown in the normal-strength concrete when fibers were added, 29.4% in moderately high-strength concrete, and 27% in high-strength concrete. "The increase in *strain* corresponding to *compressive strength* is due to the confinement effect induced by the distributed steel fibers in a concrete matrix" (Thomas & Ramaswamy, 2007). This benefit of enhanced peak *strain* capacity is a significant advantage to using FRC in blast resistant design.

This report concluded that the primary advantage of fiber reinforced concrete is in the post-cracking response, as shown below in Figure 3.3.2-1. The high-strength concrete has the greatest flexural strength gain after cracking, but all strengths show a gain in flexural strength

after cracking. The gain appears to increase as the *reinforcing index* (RI) increases; the RI is found by multiplying the fiber content by the *fiber aspect ratio*.

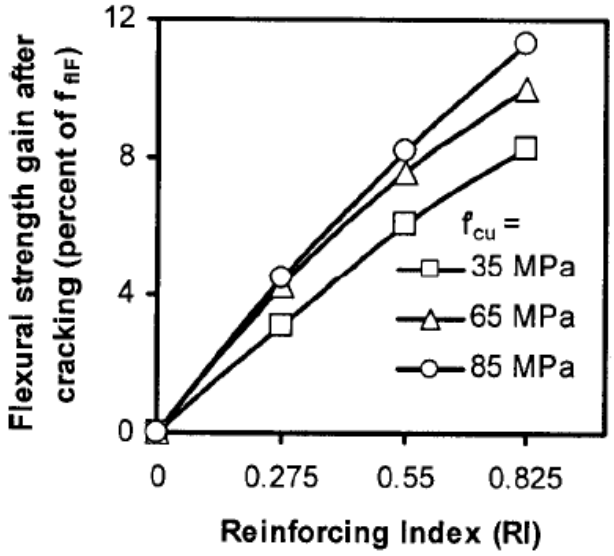

Figure 3.3.2-1 Postcracking strength enhancements in SFRC with different fiber contents for different concrete mixes (Thomas & Ramaswamy, 2007)

3.3.3 Effect of Lightweight Versus Normal Weight Concrete

The technical paper, *Correlating Flexural and Shear Toughness of Lightweight Fiber-Reinforced Concrete*, published by the ACI Materials Journal, contrasts the behavior of fiber reinforcing in lightweight and normal weight concrete, without steel reinforcing. Lightweight concrete's advantage is that it reduces the structure's dead load. However, since it is more prone to a brittle failure than normal weight concrete, it was thought to be a good candidate for adding fibers to improve its *ductility*. The behavior of FRC under shear loading was also of particular interest to the researchers, since limited research was available in this area compared to research on flexural behavior. "If a clear correlation could be established between the flexural performance and shear performance of FRC, both before and after matrix cracking, then the understanding of the performance and safety of structures subjected to high shear forces can be dramatically improved" (Higashiyama & Banthia, 2008).

The tests included mixes with two types of lightweight coarse aggregate: pumice and expansive shale. Pea gravel was used as the coarse aggregate for normal weight concrete. The

fine aggregate was river sand and the cement was general purpose portland cement. Crimped steel fibers of two different lengths, 38 mm (1.5") and 63.5 mm (2.5"), with an equivalent diameter of 1.14 mm (0.045") were used. These fibers were tested in two different fiber volumes: 0.5% and 1.0% by volume. To prevent fiber *balling*, which occurs when the fibers get congested within the concrete and aren't evenly dispersed, the fibers were added at the end of mixing.

The specimens tested were "three 100 mm x 200 mm (4" x 8") cylinders for *compressive strength* determination as per ASTM C39, three 100 mm x 100 mm x 350 mm (4" x 4" x 14") beams for determination of shear strength and *toughness* properties as per the JSCE-G 553-1999 procedure, and three 100 mm x 100 mm x 350 mm (4" x 4" x 14") beams for flexural strength and *toughness* evaluation as per ASTM C1609" (Higashiyama & Banthia, 2008). The tests followed the standards of ASTM C1609 for flexural *toughness* tests and a modified version of JSCE-G 553-1999 procedure for shear testing.

The results of the flexural testing showed that the concrete specimens with no fiber reinforcement (mixture PE-0 and PU-0) softened more rapidly, as illustrated in Figure 3.3.3-1 by the steep negative slope indicating a small deflection before failure, than the specimens with fiber reinforcing (mixture PE-5, PE-10, PU-5-38, PU 5-64, PU-10, and EX-5) which sustained loads through increasing deflection, thus responding with *ductility*.

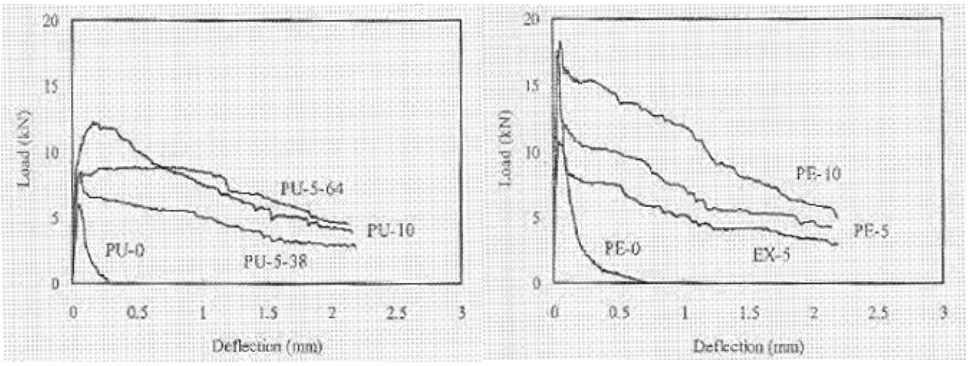

Figure 3.3.3-1 Load-deflection curves in flexure for normal weight (right) and lightweight (left) concrete (Higashiyama & Banthia, 2008)

Similar behavior was illustrated in direct shear testing, where the fiber reinforced specimens (mixture PE-5, PE-10, PU-5-38, PU 5-64, PU-10, and EX-5) showed a gradual

decrease in load carrying capacity with respect to deflection. Moreover, the unreinforced specimens without fibers (mixture PE-0 and PU-0) failed almost immediately after reaching the peak load, indicating a brittle response. The load-deflection curves in direct shear are shown below in Figure 3.3.3-2.

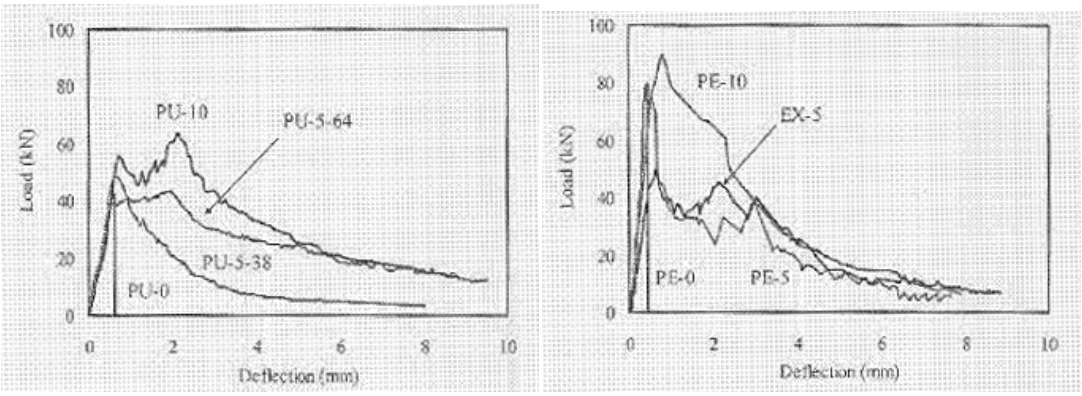

Figure 3.3.3-2 Load-deflection curves in direct shear for normal weight (right) and lightweight (left) concrete (Higashiyama & Banthia, 2008)

Comparing the flexural and shear responses shows, "greater post-peak load retention in the case of shear compared with flexure" (Thomas & Ramaswamy, 2007). The increased deflections shown in the shear testing indicates better *toughness* in shear than in flexure.

This study concluded that an increase in fiber content resulted in increased *ductility*. Also, "the post-crack shear capacity of FRC drops more sharply with an increase in the deflection (or crack opening) than [does] its flexural capacity" (Thomas & Ramaswamy, 2007). Finally, the study determined that lightweight FRC did not perform to the level of normalweight FRC during post-cracking behavior (Thomas & Ramaswamy, 2007).

4.0 Studies of FRC Under Blast Loading

Although the previous studies provided evidence to support the advantages of using fibers in reinforced concrete under impact loading, actual explosive testing of fiber reinforced members was needed to show actual behavior.

4.1 Very High-Strength Concrete for Use in Blast-and-Penetration Resistant Structures

The U.S. Army Engineer Research and Development Center conducted the study, *Very High-Strength Concrete for Use in Blast-and-Penetration Resistant Structures* (Cargile, O'Neil, & Neeley), hoping to determine a suitable concrete mix to resist the effects of blast threats. The use of very-high-strength concrete (VHSC) is of interest in this study, due to its ability to provide strength with less material, which reduces cost. The components of VHSC are the same as those for typical concrete: water, aggregate, cement, and admixtures. However, their proportions and the curing process, during which heat and pressure are applied, are the factors that produce concrete with enhanced tensile and *compressive strength*, *toughness*, and durability. The following list contains principles of VHSC:

- "Improved homogeneity through particle size and material selection"
- "Increased density by optimizing particle size and mixing technology"
- "Improved strength by maximizing reactive materials and minimizing water content"
- "Increased microstructure by applying pressure before setting and post-set heat treatment"
- "Increased tensile strength, *toughness*, and *ductility* by incorporating steel fibers or steel micro-fibers" (Cargile, O'Neil, & Neeley)

The homogeneity of particle size is one important aspect of VHSC. Since the particles have similar size and modulii, their *strain* rates are similar under loading and therefore reduce the internal tensile *strain* of the concrete. Another critical difference in VHSC versus conventional concrete is the density of the concrete. The largest aggregate used is sand, with a maximum particle size of 4.75 mm (0.187"); next, the cement particles are 10 μm (0.0004") to 100 μm (0.004") in size; finally silica fume at 0.1 μm (0.000004") is the smallest particle. The volumes of these components are carefully considered to "achieve the greatest particle packing, and hence the greatest density of the paste" (Cargile, O'Neil, & Neeley), which means a greater

ratio of solids per unit volume due to the increased efficiency in particle packing exists. The increased amount of pozzolanic material within the concrete mix for VHSC compared to that of conventional concrete also helps to increase the strength. Pozzolanic materials react with the components of the concrete to form calcium-silicate-hydrate, which acts as the "glue" between aggregates and cement. The water to cement ratio recommended for VSHC concrete is 0.4, and it is important not to exceed this ratio or else the strength of the concrete will be compromised. Only enough water is needed to react in the hydration process; any excess will weaken the compressive and tensile strengths of the concrete. However, the workability of the concrete at this water to cement ratio is difficult and therefore high-range-water-reducing admixtures must be used to make the concrete workable (Cargile, O'Neil, & Neeley).

When all these components are cured under standard conditions, no applied heat or pressure, the resulting *compressive strength* can be up to 175 MPa (25 ksi). However, if heat and pressure are applied throughout the curing process to "expel any excess liquids and air from the fresh mixture" greater strengths can be achieved (Cargile, O'Neil, & Neeley). For instance, a temperature of 90^{o}C (194^{o}F) maintained for several days throughout the curing of the concrete can generate a *compressive strength* greater than 200 MPa (29 ksi). Indeed, *compressive strength*s of at least 800MPa (116 ksi) can be reached with applied pressure and a temperature of 400^{o}C (752^{o}F) (Cargile, O'Neil, & Neeley).

To increase the tensile strength of VHSC, steel fibers are added to the mixture. "The addition of steel fibers increases the first-crack load, increases the ultimate load-bearing capacity, and dramatically increases the flexural *toughness*" (Cargile, O'Neil, & Neeley). Also, steel fibers have proven beneficial in the post cracking stage of concrete loading; "the large number of small fibers [that] cross the path of potential cracks, coupled with the good bond between fiber and matrix, provide high resistance to fiber pullout during tensile-cracking, and greatly increase the *toughness* of the material" (Cargile, O'Neil, & Neeley). Figure 4.1-1 illustrates the enhanced post-cracking behavior and *toughness* of VHSC, which is important in blast resistant design due to the expectations of members behaving into the inelastic range.

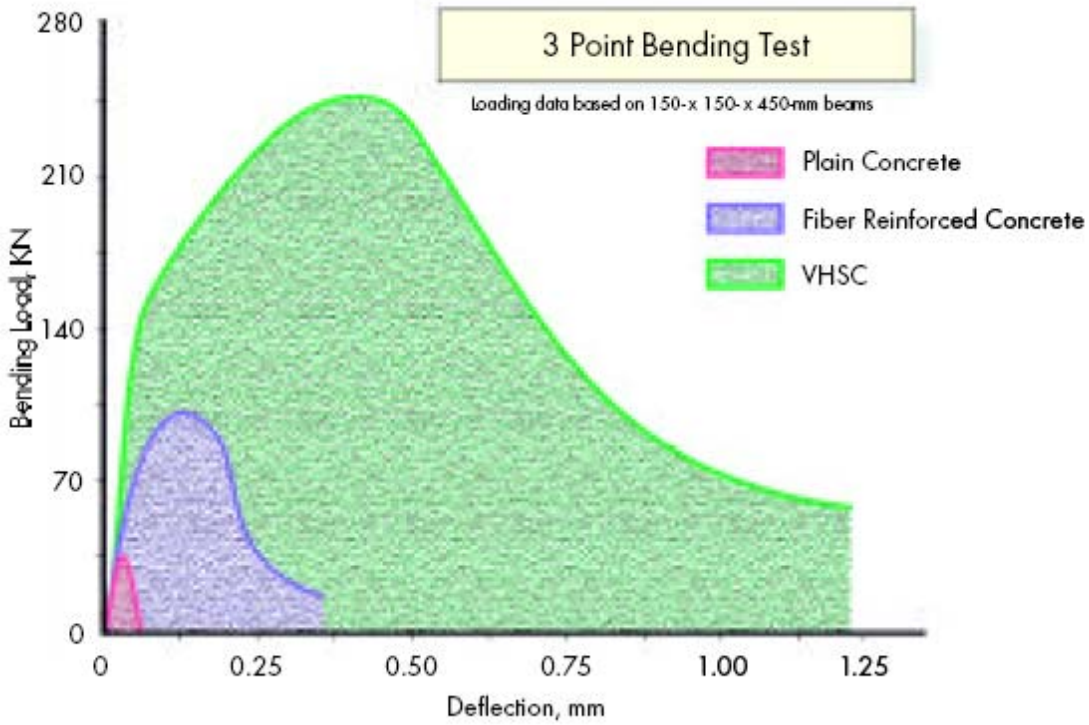

Figure 4.1-1 Flexural toughness comparison for VHSC Concrete vs. plain and fiber-reinforced concrete (Cargile, O'Neil, & Neeley)

Toughness, "a measure of the amount of energy that must be expended to open cracks in the matrix under tensile loading," is a critical property in resisting blast loading (Cargile, O'Neil, & Neeley). Researchers expect that the VHSC will either stop the projectile from penetrating the member, reduce spalling from the back face of the member, or slow the velocity of the projectile leaving the member to less than would be likely with conventional concrete (Cargile, O'Neil, & Neeley).

The steel fibers for this study were hooked-end with a diameter of 0.5 mm (0.0197") and a length of 30 mm (1.18"). These fibers were shown to be most effective and economical in previous studies (Cargile, O'Neil, & Neeley).

To achieve the desired concrete strength, the concrete "targets," 914 mm (36") long and 762 mm (30") wide, were wrapped in insulation to keep the temperature high. To maintain moisture, water was ponded on the surface for a week. After that, the concrete was cured in ambient conditions and allowed to cure 30 to 60 days before being tested.

Next, testing compared the depth of penetration into the concrete at the velocity at which a projectile was traveling upon impact. The projectiles weighed 0.906 kg (2 lbs) and had a diameter of 26.9 mm (1.1") and an overall length of 242.4 mm (9.54"). They were projected from "the ERDC (formally WES) 83-mm (3.27"), smooth-bore powder gun at striking velocities (V_s) ranging from 229 m/s (751 feet/s) to 754 m/s (2,474 feet/s)" (Cargile, O'Neil, & Neeley).

Four different mixes of concrete were compared: conventional-strength portland cement concrete (CSPC), high-strength portland cement concrete (HSPC), high-strength, steel-fiber reinforced concrete (HSFR), and very-high-strength concrete (VHSC), which included steel fibers in its mix. Notably, the VHSC mix was the only one in this particular study to be compared to the three other mixes already tested under similar constraints. The hardened material properties of the four mixes are provided in Table 4.1-1, which shows VHSC has the highest strengths of the four mixes, with a 450% increase in *compressive strength* over CSPC, 150% increase over HSPC, and 185% increase over HSFR. In regards to the compressive *modulus of elasticity*, the percent increases of VHSC compared to CSPC, HSPC, and HSFR are 133%, 102%, and 102%, respectively. Significantly, the percent increase of tensile strength for VHSC compared to CSPC, HSPC, and HSFR are 257%, 188%, and 200%, respectively.

Table 4.1-1 Hardened material properties (Cargile, O'Neil, & Neeley)

	CSPC	HSPC	HSFR	VHSC
28-day Compressive Strength, (MPa)	35	104	85	157
Compressive Modulus of Elasticity, (GPa)	34.5	45.2	45.2	46
56-day Tensile Strength, (MPa)	3.5	4.8	4.5	9.0
Tensile Modulus of Elasticity, (GPa)	44	39.5	39.6	–

The results of the penetration experiments with VHSC were compared to those of previous experiments using CSPC, HSPC, and HSFR and showed that the VHSC performed as expected, with the least depth of penetration versus striking velocity of the four mixes. This is important because a lower depth of penetration indicates higher energy absorption at striking velocity. A graph of these results is shown in Figure 4.1-2.

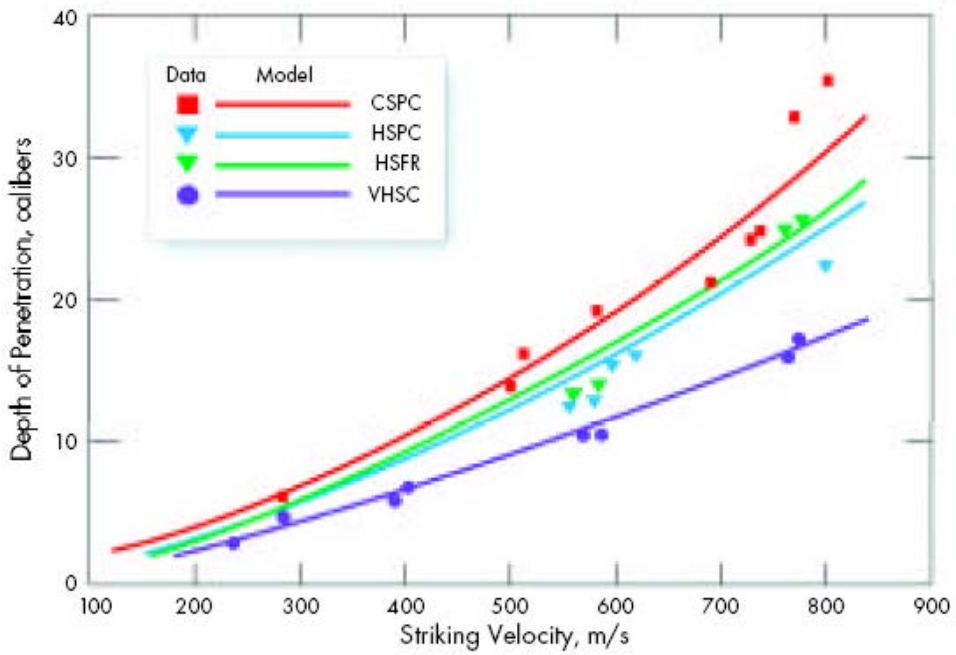

Figure 4.1-2 Comparison of penetration experiment results and spherical-cavity expansion model calculations for CSPC, HSPC, HSFR, and VHSC concretes (Cargile, O'Neil, & Neeley)

The method for calculating the model depth of penetration was a "spherical-cavity expansion model developed by Forrestal and Tzou" (Cargile, O'Neil, & Neeley). This method takes into account "density, yield strength, slope of the yield surface, tensile strength, and linear bulk modulus" to determine the depth of penetration versus striking velocity behavior. These properties influence the specimen's response to projectile penetration. As shown in Figure 4.1-2, the prediction of the model agreed with the experimental data, which is a significant step towards blast resistant design, when model predictions can yield results which are similar to actual results (Cargile, O'Neil, & Neeley).

The results showed that the penetration into VHSC is about half that of penetration into CSPC. Additionally, the results of the HSFR concrete test showed a "significant decrease in visible damage, and still resulted in a depth of penetration about 30% less than [that of] the CSPC," but fiber addition alone did not reduce projectile penetration depth, as the HSPC had a similar depth of penetration (Cargile, O'Neil, & Neeley). Ultimately, researchers concluded that VHSC was successful in "spall resistance and increased deflection without failure and exhibited a flexural *toughness* "greater than 250 times that of conventional, non-fiber-reinforced concrete", which improves reinforced concrete's ability to meet the blast resistant design goals of preventing collapse of the structure and reducing flying debris (Cargile, O'Neil, & Neeley). It should be noted that while VHSC was mechanically successful, the curing process used for this experiment, including insulating wraps and water ponding, would be labor intensive for field construction and therefore, an impractical material choice at this time.

4.2 Blast Testing of Ultra-High Performance Fiber and FRP-Retrofitted Concrete Slabs

The University of Adelaide, in Australia, conducted a study, *Blast Testing of Ultra-High Performance Fiber and FRP-Retrofitted Concrete Slabs,* to find a material "to mitigate the effects of blast loads on buildings" (Wu, Oehlers, Rebentrost, Leach, & Whittaker, 2009). The material tested was another *high strength concrete*; "Ultra-high performance fiber concrete (UHPFC) is a relatively new construction material with higher strength, deformation capacity and *toughness* than conventional normal strength, normal weight concrete" (Wu, Oehlers, Rebentrost, Leach, & Whittaker, 2009). The mix for this type of concrete includes steel fibers to enhance the strength and *ductility* characteristics. In Figure 4.2-1 "Sample *stress-strain* curves for UHPFC materials are shown", illustrating the enhanced *ductility* of the UHPFC through increased *stress* capacity at increased *strain*s, with a gradual decrease in *stress* capacity with increasing *strain* for both compressive and tensile *stresses* (Wu, Oehlers, Rebentrost, Leach, & Whittaker, 2009).

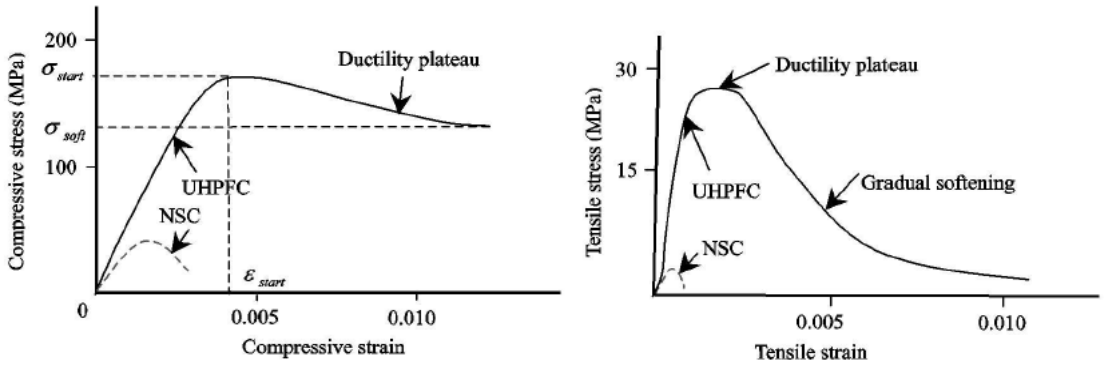

Figure 4.2-1 Mechanical properties of conventional concrete and UHPFC (Wu, Oehlers, Rebentrost, Leach, & Whittaker, 2009)

This study's objective was to explore the response of UHPFC under blast loading. The control specimens were made with normal reinforced concrete (NRC) that had two layers of wire mesh reinforcing, one for the tension face and one for the compression face. The wire mesh had a diameter of 12 mm (.47") and a spacing of 100 mm (3.9") in the major bending direction and a spacing of 200 mm (7.9") in the minor bending direction. "The concrete had a cylinder *compressive strength* of 39.5 MPa (5.7 ksi), tensile strength of 8.2 MPa (1.2 ksi) and *Young's modulus* of 28.3 GPa (4,105 ksi)" (Wu, Oehlers, Rebentrost, Leach, & Whittaker, 2009). Two specimens of UHPFC were cast for testing: one with reinforcing bars in addition to the fiber reinforcing (RUHPFC) and one without (UHPFC). The UHPFC strengths were found to be 151.6 MPa (22 ksi) for the average *compressive strength*, which is an increases of 386% compared to the NRC, 30.2 MPa (4.4 ksi) for the tensile strength, which is an increase of 367% compared to the NRC, and 47 GPa (6,820 ksi) for *Young's modulus*, which is an increase of 166% compared to the NRC (Wu, Oehlers, Rebentrost, Leach, & Whittaker, 2009).

A steel frame was used to prevent lateral movement and restrained the slabs from the suction force from the negative phase of the blast wave. Figure 4.2-2 illustrates this test set-up. A frame consisting of pipe sections was constructed to support the explosive charge. "The charge was suspended from the horizontal section with light rope. The charge was centered over the slab using four string guides" (Wu, Oehlers, Rebentrost, Leach, & Whittaker, 2009).

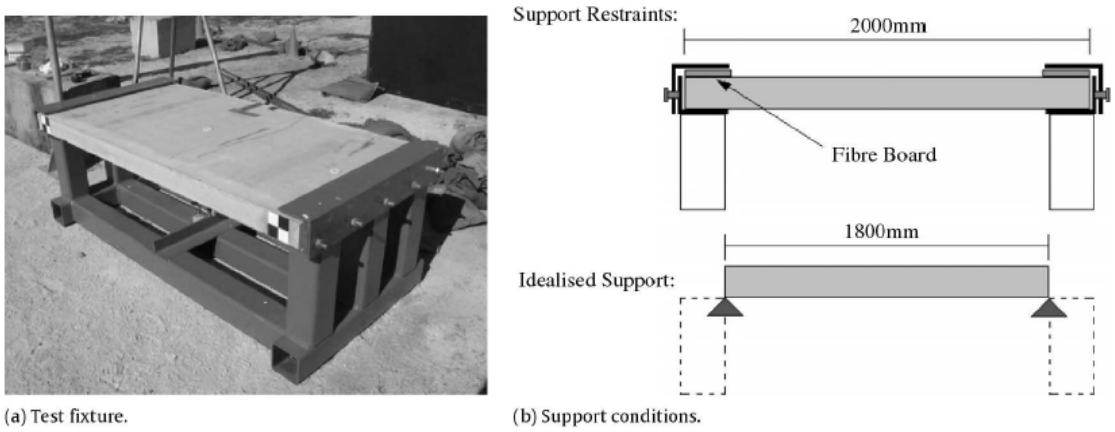

Figure 4.2-2 Support conditions for slab testing (Wu, Oehlers, Rebentrost, Leach, & Whittaker, 2009)

To record the data during testing, "a Linear Variable Displacement Transducer (LVDT), pressure transducers, and a high speed camera" were used (Wu, Oehlers, Rebentrost, Leach, & Whittaker, 2009). Specifically, a pressure transducer recorded pressures at the center of the slab, and one recorded pressures near the support. (Wu, Oehlers, Rebentrost, Leach, & Whittaker, 2009)

The explosives used for testing were cylindrically shaped, and the diameter equaled the length. Previous studies had determined that the shape and diameter to length ratios played an important role in the detonation results. One conclusion was that "for low ratios of length-to-diameter, more energy is directed in the axial direction [,] and for high length-to-diameter ratios, more energy is directed in the radial direction" (Wu, Oehlers, Rebentrost, Leach, & Whittaker, 2009). After testing, researchers compared the experimental overpressures and impulses to the pressures and impulses predicted by the Department of Defense document, *Structures to Resist the Effect of Accidental Explosions*, TM5-1300, which showed that the majority of the experimental values exceeded the predicted values. The reason for this discrepancy is attributed to the small standoff distance, the length-to-diameter ratio, and the cylindrical shape of the explosive charge (Wu, Oehlers, Rebentrost, Leach, & Whittaker, 2009).

The factors and results of the blast load on the concrete slabs are summarized in Table 4.2-1. Clearly, as discussed in *Section 2.0 Blast Resistant Design*, charge weight and standoff distance dramatically influence the pressures experienced by the slabs, therefore, the maximum deflection of the slabs indicates the amount of energy absorption. The first four tests listed were

conducted on normal reinforced concrete (NRC) slabs. The first two tests, NRC-1 and NRC-2, showed no cracking in the specimens after testing. However, blast NRC-3 showed minor flexural cracking, indicating that pressures from this blast did not exceed the yield moment. Figure 4.2-3 illustrates the crack pattern from NRC-3.

Table 4.2-1 Summary of slab deflections (Wu, Oehlers, Rebentrost, Leach, & Whittaker, 2009)

Blast	Charge weight (kg)	Standoff distance from PT1 (m)	Scaled distance ($m/kg^{1/3}$)	Max. deflection (mm)	Permanent deflection (mm)
NRC-1	1	3	3	1.5	0
NRC-2	8	3	1.5	10.5	–[a]
NRC-3	3.4	1.4	0.93	13.9	–[a]
NRC-4	8	1.5	0.75	38.9	–[a]
RET-1	1	1.5	1.5	3.3	0
RET-2	5	0.92	0.54	50.6	7.6
UHPFC	3.4	0.75	0.5	13.2	4.1
RUHPFC	20	1	0.37	>100	–[b]

[a] LVDT debonded from the concrete and the permanent deflection was not recorded.
[b] LVDT was destroyed by the test.

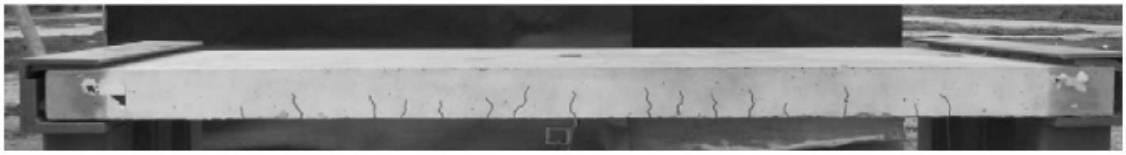

Figure 4.2-3 Cracks in specimen NRC-3 (Wu, Oehlers, Rebentrost, Leach, & Whittaker, 2009)

The final test on normal reinforced concrete, NRC-4, used the strongest blast of the four tests based on a large charge weight being detonated at the shortest standoff distance. The results of this test showed significant cracks; "residual crack widths were measured, indicating a plastic or post-yield response" (Wu, Oehlers, Rebentrost, Leach, & Whittaker, 2009). Figure 4.2-4 illustrates the crack pattern from NRC-4, which consists of flexural cracking with greater widths than NRC-3.

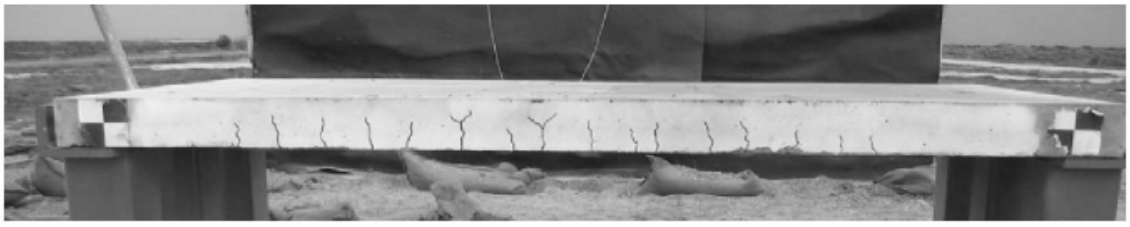

Figure 4.2-4 Cracks in specimen NRC-4 (Wu, Oehlers, Rebentrost, Leach, & Whittaker, 2009)

The next two tests, RET-1 and RET-2, were performed on retrofitted reinforced concrete slabs. The placement of FRP plates on the compression face of the concrete slabs is a configuration that is outside the scope of this report, however, the results of these tests reveal much about the behavior of concrete slabs subjected to blast loads. RET-2 had a relatively large charge weight at a relatively small standoff distance, which caused shear cracks to form. "During rapid loading, direct shear cracks can be formed in areas of concentrated loads. Direct shear failures will preclude the development of the strength of a slab and are undesirable, although, probably unavoidable for near-field charges" (Wu, Oehlers, Rebentrost, Leach, & Whittaker, 2009). A photograph of this slab and the resulting crack patterns is presented in Figure 4.2-5, where it is apparent that shear cracks were formed near the support and flexural cracks were formed midspan, which was the expected response.

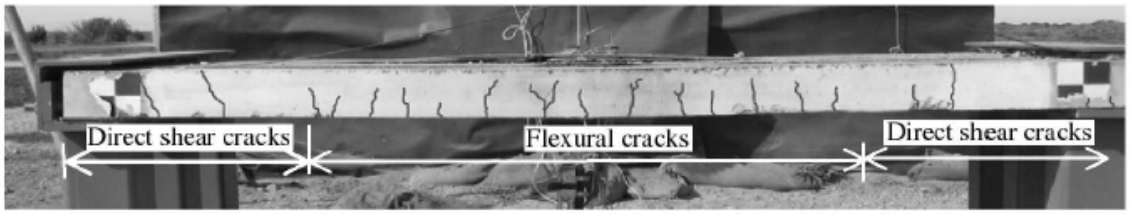

Figure 4.2-5 Crack pattern in RET-2 (Wu, Oehlers, Rebentrost, Leach, & Whittaker, 2009)

The next test was performed on ultra-high performance fiber concrete without reinforcing. At a charge weight of 3.4 kg (7.5 lbs) and a standoff distance of 0.75 m (29.5"), this represented the smallest explosive of all the tests; it showed flexural cracking but not shear

cracking. "This test confirmed the substantial ability of ultra-high performance fiber concrete for resisting blast loads" (Wu, Oehlers, Rebentrost, Leach, & Whittaker, 2009).

The last test was performed on reinforced ultra-high performance fiber concrete. The charge weight of the explosive was more than twice the size of the largest charge weight used in the tests. Additionally, the standoff distance was only 1 m (39.4") making this blast "approximately 15 – 20 times greater" than the other blasts (Wu, Oehlers, Rebentrost, Leach, & Whittaker, 2009). The response of this slab was characterized by crushing of concrete on the top surface near the midspan of the slab however, little spalling and no shear cracking was observed. A photograph of the slab after testing is presented in Figure 4.2-6**.** "The usefulness of ultra-high performance fiber concrete for blast resistance was further confirmed by this large blast load at a small standoff distance." (Wu, Oehlers, Rebentrost, Leach, & Whittaker, 2009)

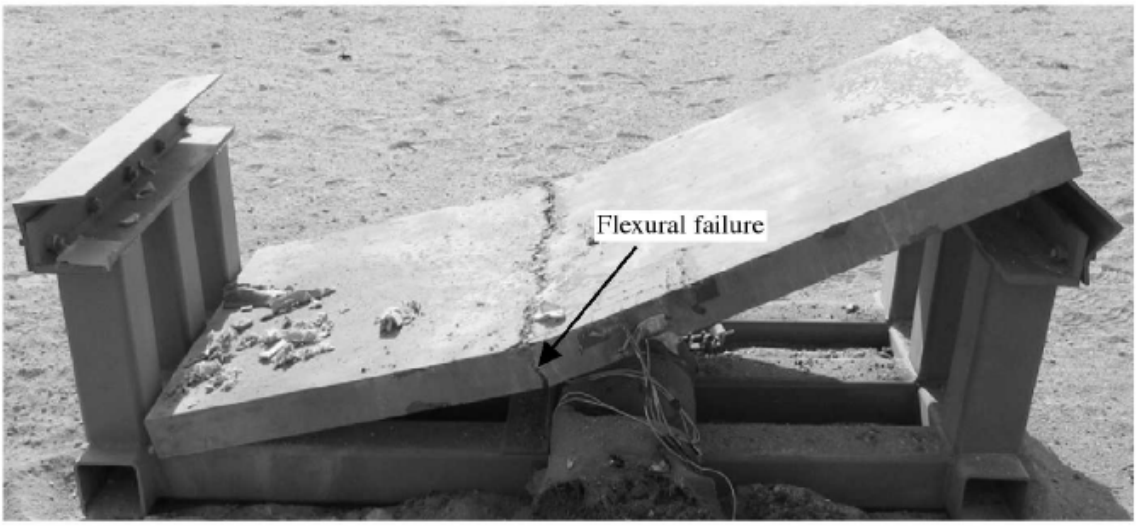

Figure 4.2-6 Flexural failure of the RUHPFC specimen (Wu, Oehlers, Rebentrost, Leach, & Whittaker, 2009)

The capacity of a specimen to absorb energy, quantified by finding the area under the resistance-deflection curve, is useful for evaluating the test results. First, the loading was considered impulsive, since the duration of the load was measured to be between 0.99 ms and 1.70 ms. Thus, the energy absorption capacity, E_n, is found by Equation 4.2-1:

$$E_n > \frac{I^2}{2(K_{LM}M)} \qquad \text{Equation 4.2-1}$$

Where I is the applied impulse, K_{LM} is the load-mass transformation factor, and M is the mass of the slab. It was stated that "the value of K_{LM} for a SDOF system for a simply supported member subjected to a uniformly distributed load and responding far into the inelastic range is 0.72" (Wu, Oehlers, Rebentrost, Leach, & Whittaker, 2009). This value was obtained from the textbook, *Introduction to Structural Dynamics* by J. Biggs. Next, I, is the averaged reflected impulse measured during testing for NRC-1, NRC-2, NRC-3, and RET-1, or computed from the Navy and Air Force Technical Manual, TM5-1300, for all other specimens. These specimens did not have recorded experimental reflected impulses due to the limit of the pressure sensors at 6.9 MPa (1000 psi). Therefore, the mass of all specimens was determined to be approximately 440 kg (970 lbs), which was used for calculations. The applied impulse energy was computed and is presented in Table 4.2-2. Also included in this table are values for the predicted energy absorption capacity, estimated energy absorption, and averaged reflected impulse. Clearly, RUHPFC specimen had the highest predicted energy absorption capacity and the applied impulse energy exceeded this value by almost a factor of three (Wu, Oehlers, Rebentrost, Leach, & Whittaker, 2009).

Table 4.2-2 Resistance, reflected impulses and energy demands, and capacities (Wu, Oehlers, Rebentrost, Leach, & Whittaker, 2009)

Specimen	Charge weight (kg)	Scaled distance ($m/kg^{1/3}$)	Predicted energy absorption capacity (kN mm) E_n	Recorded max. deflection (mm)	Estimated energy absorption (kN mm)	Averaged reflected impulse (kN ms)	Applied impulse energy (kN mm) $\frac{I^2}{2(K_{LM}M)}$
NRC-1	1.0	3.00	3725	1.5	33	287	141
NRC-2	8.0	1.50	3725	10.5	1630	1106	2124
NRC-3	3.4	0.93	3725	13.9	2572	1209	2536
RET-1	1.0	1.50	6730	3.3	192	599	624
NRC-4	8.0	0.75	3725	38.9	$>E_n$	1774	5464
RET-2	5.0	0.54	6730	50.6	$>E_n$	2445	10375
UHPFC	3.4	0.75	2194	13.2	$>E_n$	1335	3089
RUHPFC	20.0	1.00	32339	>100	$>E_n$	7322	93077

The flexural blast resistance was determined by dividing the slab cross section into layers and then assuming the *strain*, rate, and *stress* to be constant in each layer. The resistance of each layer was determined considering the *stress*, *dynamic increase factor*, width, and thickness of the layer. Once the *neutral axis* was determined, the moment capacity could be calculated. The energy absorption capacities of the retrofitted concrete slabs and the normal reinforced concrete slabs were determined in a previous study, "Layered Blast capacity Analysis of FRP Retrofitted RC Members" by the same authors (Wu, Oehlers, Rebentrost, Leach, & Whittaker, 2009).

The derivation of the moment curvature diagram for RUHPFC is shown below in Figure 4.2-7. Clearly, section A of the moment curvature graph illustrates a linear relationship, defining the behavior as linear elastic. Section B occurs after the steel has yielded, indicating that the concrete tensile capacity has been exceeded. In this section an increased *stress* in the tensile portion of the cross section is evident due to the tensile capacity of the fibers in the concrete, which moves the location of the *neutral axis* up towards the compression region as illustrated in Figure 4.2-8. This reduces the moment capacity of the section also shown in Figure 4.2-7.

The behavior of section C "starts when the compressive *stress* reaches its maximum value at the extremity" (Wu, Oehlers, Rebentrost, Leach, & Whittaker, 2009). Thus, as section C of the moment curvature graph progresses, the compression block reaches its maximum compressive strength from the extreme fiber towards the *neutral axis*, until failure is caused by crushing, which is illustrated in Figure 4.2-8.

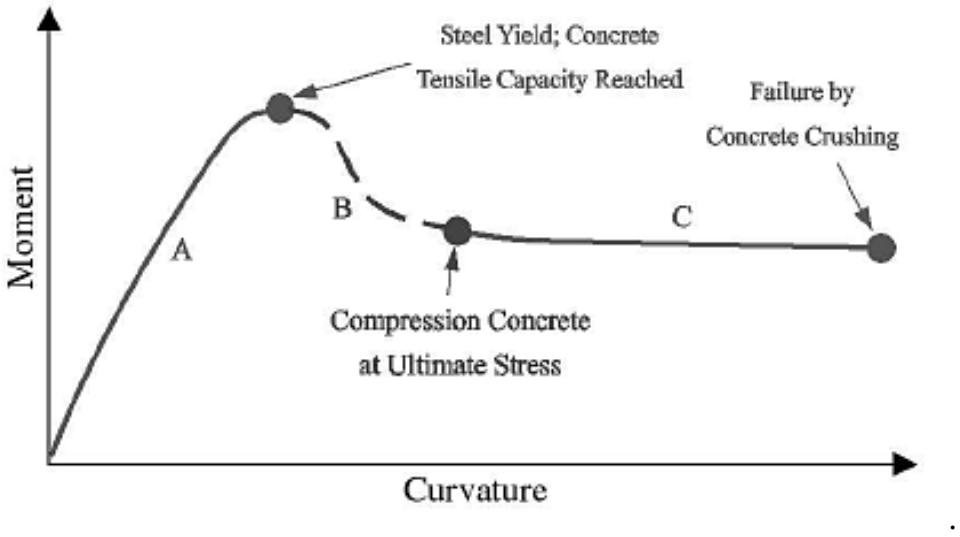

Figure 4.2-7 Moment-curvature relationship for RUHPFC specimen (Wu, Oehlers, Rebentrost, Leach, & Whittaker, 2009)

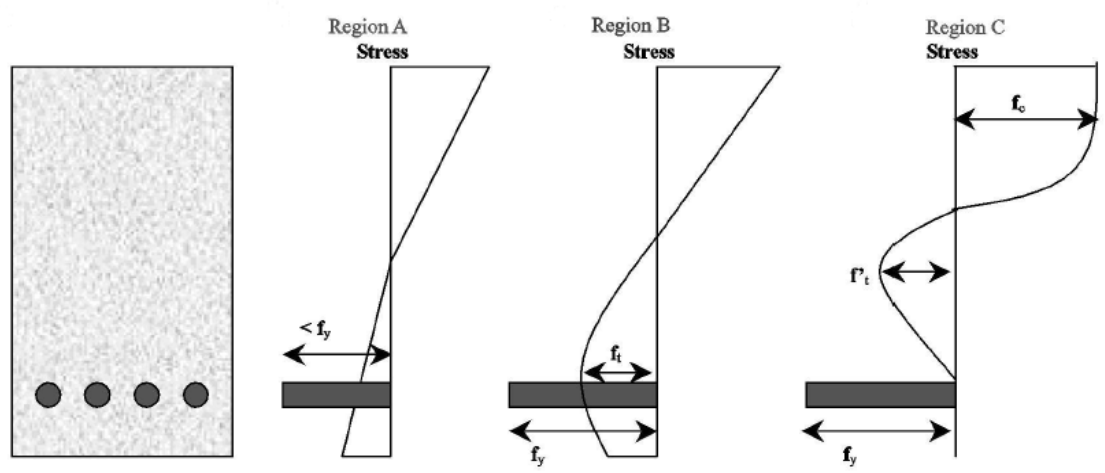

Figure 4.2-8 Stress profiles for different regions of the moment-curvature of RUHPFC specimen (Wu, Oehlers, Rebentrost, Leach, & Whittaker, 2009)

This study shows that the RUHPFC was the preferable concrete mixture for resisting blast loads, as it has the highest energy absorption capacity. “Importantly no scabbing or shear cracking was observed in the RUHPFC slab after testing with a large weapon at close range,” which means less flying debris (Wu, Oehlers, Rebentrost, Leach, & Whittaker, 2009). Additionally, researchers noted that the UHPFC slabs performed better by suffering less damage than the NRC slabs when exposed to similar explosive charge weights (Wu, Oehlers, Rebentrost, Leach, & Whittaker, 2009). The results of this study show that adding fibers, whether to the RUHPFC or the UHPFC mix, is beneficial to the behavior of the concrete under blast loading.

5.0 Limitations of SFRC

Although promising research that supports the use of steel fibers in reinforced concrete exists, a few limitations to its use in design are: cost, mixing and placing, and corrosion of surface fibers.

5.1 Cost of SFRC

If steel fiber reinforced concrete is accepted into industry as a blast resistant material, cost is an issue that must be addressed. While SFRC is currently used in the construction industry, its applications are at a relatively low volume, such as slabs. If SFRC is used as a blast resistant material for structures, the material cost of adding fibers could be substantial. Therefore, some estimates from the Kansas City area from William R. "Rusty" Owings III at Ash Grove KC Concrete Group are used as an example. The current cost of 27.6 MPa (4000 psi), Type I/II cement, exterior use concrete is $88.00 per yard and $53.00 per 20 kg (44 lbs) bag of hooked end steel fibers. The concrete type and strength were simply chosen because of their common usage. These costs do not include additional labor or admixtures.

Based on the mix proportions used by the study, *Mechanical Properties of Steel Fiber Reinforced Concrete Beams*, the addition of fiber, with a fiber percentage of 0.5 by volume, would cost approximately $10.00 more per yard. Clearly, a fiber percentage of 1.5 by volume would cost approximately $30.00 more per yard. Using the cost of concrete of $88.00 per yard given above, means that the addition of fibers at a percentage of 0.5 by volume results in an 11% increases in cost and a fiber percentage of 1.5 by volume results in a 34% increase in cost. As the strength of concrete increases, so does the price, which means the percent increase in cost would decrease with concrete strength, but overall cost would increase.

These estimations are only provided to give a general idea of expected cost increases with the addition of steel fibers to concrete mixes. However, several additional considerations must be taken into account: fiber type, fiber dosage, concrete strength, regional cost indexes, additional labor before an accurate cost estimate can be arrived at.

5.2 Mixing of SFRC

Adding steel fibers to a concrete mix can create problems with mixing and placing the concrete. "The large surface area of fibers tends to restrain flowability and mobility of the mix"

(Bayasi & Soroushian, 1992). In particular, fiber *balling* can occur when fibers interlock within the concrete mix, therefore reducing the workability and compromising the material properties of the hardened concrete (Bayasi & Soroushian, 1992).

Specifically, three fiber properties affect the workability of the concrete are: percent of fibers by volume, length-to-diameter ratio, and shape. Clearly, increasing the amount of fibers increases the potential for problems with fresh mix workability. Also, increasing the length-to-diameter ratios, while beneficial in post-peak performance for resisting pullout, can have an adverse effect on fresh mix workability (Bayasi & Soroushian, 1992). Next, the recommended length-to-diameter ratio is between 50 and 100; at 100 or above, fiber interlocking is likely to occur, and at 50 or below, the mechanical properties, specifically tensile strength, of the concrete are compromised because the length of the fiber is too short to effectively resist pullout from the concrete matrix, similar to the development length of steel reinforcement in concrete. To increase the fiber's resistance to pullout, fibers can be deformed (ACI Committee 544, 1996). However, the shape of the fibers, crimped, hooked, or straight, for example, influences the air content of the mixture. Tests showed that deformed fibers increased the air content, thereby decreasing the workability of the mixture (Bayasi & Soroushian, 1992).

Furthermore, aggregate size affects the potential for fiber *balling*. "The larger the maximum size aggregate and aspect ratio, the less volume fraction of fibers can be added without the tendency to ball" (ACI Committee 544, 1996). Guidelines for determining mix proportions in relation to maximum aggregate size ($^3/_8$", ¾", and 1 ½") are given Table 2.2 of the ACI 544.1 R-96 document, *Fiber Reinforced Concrete*.

While testing by Bayasi and Soroushian found that adding fibers decreases slump, the ACI 544.1 R-96 document, *Fiber Reinforced Concrete* notes that it does "not necessarily mean that there is a corresponding loss of workability, especially when vibration is used during placement" (ACI Committee 544, 1996). To accurately measure workability, the report, suggests "the inverted slump cone test (ASTM C 995) or the Vebe Test (BS 1881)" (ACI Committee 544, 1996). Ultimately, careful consideration of fiber volume, length-to-diameter ratios, shape, and maximum aggregate size coupled with admixtures that address "air entrainment, water reduction, workability, and shrinkage control," can enable engineers and

contractors to overcome the mixing and placing challenges of fiber reinforced concrete (ACI Committee 544, 1996).

5.3 Corrosion of SFRC

Although most fibers "are protected from corrosion by the alkaline environment of the cementitious matrix," exposed steel fibers can corrode (ACI Committee 544, 1996). Fortunately, even given corrosion of the surface fibers, corrosion does not penetrate more than 2.54 mm (0.10") below the surface of the uncracked concrete. However, if the concrete is cracked, and the cracks are greater than 0.1 mm (0.004") wide, corrosion can extend to the fibers exposed across the crack. This corrosion, depending on how critical the location of the corrosion is, could have a significant effect on the structural stability during blast loading.

"Most of the corrosion testing of SFCR has been performed in a saturated chloride environment, whether experimentally in the laboratory or in a marine tidal zone". ACI 544.1 R-96 states that "corrosion behavior of SFRC in aggressive non-saturated environment or in fresh water exposure is limited" (ACI Committee 544, 1996). Thus, while corrosion may not be a significant deterrent to using steel fibers in reinforced concrete, it does require some design consideration. Alternatives such as stainless steel fibers, alloyed carbon steel fibers, or galvanized carbon steel fibers are available if corrosion is expected to be a problem, but further research on their mechanical properties would need to be investigated before they could be used as a subsititute (ACI Committee 544, 1996).

6.0 Conclusion

Reinforced concrete is clearly a desirable material choice for blast resistant design. The first step to designing a blast resistant reinforced concrete structure is to implement proper detailing, which includes the addition of steel reinforcement in typical compression regions that could experience tensile forces due to load reversals experienced during blast loading, to ensure the structure performs in the best possible, most controlled manner. This does not mean the structure will not experience failures, but that the failure will be contained in a way that preserves as many lives as possible. To design for such preservation requires a list of priorities. Logically, preventing the building from collapse is the first of these priorities, and adding steel fibers to concrete has been shown through testing to enhance the concrete's post-crack behavior, which addresses this priority. The second priority is reducing flying debris; studies have shown that the delayed failure mechanisms of steel fiber reinforced concrete better reduce flying debris than conventional reinforced concrete exposed to blast loading.

The major considerations in designing steel fiber reinforced concrete for blast resistance include the strength level of the concrete, fiber volume fraction, and fiber shape. As research on this topic progresses, the understanding of these factors and how they affect the strength characteristics of the concrete will increase, and acceptance into building codes will be possible.

Though some limitations exist to adding steel fibers to reinforced concrete exist, such as additional cost, potential for corrosion, and difficulty in mixing and placement, thoughtful consideration during design and construction can overcome these limitations.

7.0 Works Cited

ACI Committee 544. (1996). *Fiber Reinforced Concrete.* Farmington Hills, MI: American Concrete Institute.

Agnew, E., Marjanishvili, S., & Gallant, S. (2007, January). Concrete Detailing for Blast. *Structure Magazine* , pp. 26-28.

Applications . (2007). Retrieved February 10, 2010, from Fiber Reinforced Concrete Association: http://fiberreinforced.org

Bayasi, M. Z., & Soroushian, P. (1992). Effect of Steel Fiber Reinforcement on Fresh Mix Properties of Concrete. *ACI Materials Journal* , 369-374.

Cargile, J. D., O'Neil, E. F., & Neeley, B. D. (n.d.). Very-High-Strength Concretes for Use in Blast-and-Penetration-Resistant Structures. *AMPTIAC Quarterly* , 61-66.

Galinat, M. A. (2007). Fibers for Blast Resistance. *PCI Journal* , 51-52.

Higashiyama, H., & Banthia, N. (2008). Correlating Flexural and Shear Toughness of Lightweight Fiber-Reinforced Concrete. *ACI Materials Journal* , 251-257.

Hinman, E. (2003). *Primer for Design of Commercial Buildings to Mitigate Terrorist Attacks.* FEMA 427.

Lane, R., Craig, B., & Babcock, W. (2002). Materials for Blast and Penetration Resistance. *The AMPTIAC Quarterly* , 39-45.

Lok, T., & Xiao, J. (1999). Steel-Fibre-Reinforced Concrete Panels Exposed to Air Blast Loading. *Institution of Civil Engineers Structures and Buildings* , 319-331.

McCann, D. M., & Smith, S. J. (2007, April). Blast Resistant Design of Reinforced Concrete Structures. *Structure Magazine* , pp. 22-26.

Millard, S., Molyneaux, T., Barnett, S., & Gao, X. (2010). Dynamic Enhancement of Blast-Resistant Ultra High Performance Fibre-Reinforced Concrete Under Flexural and Shear Loading. *International Journal of Impact Engineering* , 405-413.

Owings, W. R. (2010, April 6). Steel Fiber Estimate. Overland Park, Kansas, United States of America.

Suaris, W., & Shah, S. (1983). Properties of Concrete Subjected to Impact. *J. Struct. Engrg.* , 1727-1741.

Tadepalli, P., Mo, Y., Hsu, T., & Vogel, J. (2009). Mechanical Properties of Steel Fiber Reinforced Concrete Beams. *2009 Structures Congress* (pp. 1039-1048). Austin, TX: ASCE.

Thomas, J., & Ramaswamy, A. (2007). Mechanical Properties of Steel Fiber-Reinforced Concrete. *Journal of Materials in Civil Engineering* , 385-392.

Wu, C., Oehlers, D., Rebentrost, M., Leach, J., & Whittaker, A. (2009). Blast Testing of Ultra-High Performance Fibre and FRP-Retrofitted Concrete Slabs. *Engineering Structures* , 2060-2069.

Appendix A - Glossary of Terms

Balling - "When fibers entangle into large clumps" (ACI Committee 544, 1996).

Compressive strength – "The compressive strength of concrete is determined by testing to failure 28-day-old 6" by 12" concrete cylinders at a specified rate of loading" (McCormac & Nelson, 2006).

Ductility – As load is applied material deforms significantly before failure. Also an indication of energy absorption capacity of a material.

Dynamic increase factor (DIF) – Value that takes into account increased "strength and modulus of elasticity of the constitutent materials (concrete and steel fiber considered separately), as well as the bond strength between the steel fiber and concrete (acting coherently" when subjected to a high loading rate, such as a blast (Lok & Xiao, 1999).

Fiber Aspect Ratio – "The ratio of length to diameter of the fiber" (ACI Committee 544, 1996).

Flexural toughness – "The area under the flexural load-deflection curve obtained from a static test of a specimen up to a specified deflection. It is an indication of the energy absorption capability of a material" (ACI Committee 544, 1996).

High Strength Concrete – "Concretes with compression strengths exceeding 6000 psi"; also referred to as high-performance concretes (McCormac & Nelson, 2006).

Modulus of elasticity – Slope of the linear portion of the stress-strain curve. "The higher the value, the smaller the deformations in a member" (McCormac & Nelson, 2006).

Modulus of rupture (MOR) - "The greatest bending stress attained in a flexural strength test of a fiber reinforced concrete specimen. Although modulus of rupture is synonymous with matrix cracking for plain concrete specimens, this is not the case for fiber reinforced concrete specimens" (ACI Committee 544, 1996).

Neutral Axis – Location in cross section, perpendicular to loading, where internal stress is zero.

Poisson's ratio – Ratio of lateral expansion to longitudinal shortening experienced during compressive loading (McCormac & Nelson, 2006).

Reinforcing Index (RI) – Value that takes into account fiber volume and fiber length (Thomas & Ramaswamy, 2007).

Split tensile strength – Tensile strength at which a testing specimen, typically a cylinder, splits when compressive loads are "applied uniformly along the length of the cylinder, with support supplied along the bottom for the cylinder's full length" (McCormac & Nelson, 2006).

Strain – Found by dividing the longitudinal deformation of a member by its length.

Stress – "The force per unit area, or intensity of the forces distributed over a given section" (Beer, Johnston Jr., & DeWolf, 2006).

Toughness - "Total energy absorbed in breaking a member in flexure" (McCormac & Nelson, 2006).

Young's modulus – See "Modulus of Elasticity"

Appendix B - Copyright Permission

Subject: FW: Copy Right Permission

Sent By "Richard A Lane" <RLane@alionscience.com> On: April 8, 2010 10:41 AM

To: dkalman@k-state.edu

Dear Ms. Kalman,

You may copy the figures and tables into your report, as long as re-print permission is cited on the figures and tables, with recognition given to AMPTIAC. (note: AMPTIAC was consolidated with two other IACs in 2006 into what is now AMMTIAC).

Regards,

Richard A. Lane
Mechanical Engineer
Advanced Materials, Manufacturing and Testing Information Analysis Center
201 Mill St.
Rome, NY 13440
Office: 315-339-7097
Fax: 315-339-7107
ammtiac.alionscience.com

-----Original Message-----
From: Deidra Kalman [mailto:dkalman@k-state.edu]
Sent: Thursday, April 08, 2010 11:24 AM
To: Grethlein, Christian E
Subject: Copy Right Permission

Mr. Grethlein,
I am a graduate student at Kansas State University and am referencing the article, Very-High-Strength Concretes for Use in Blast-and Penetration-Resistant Structures by Dr. J. Donald Cargile, Ed F. O'Neil and Billy K. Neeley from the AMPTIAC Quarterly, Volume 6, Number 4 for my Master's Report. I was wondering what the procedure is to obtain permission to use figures and tables from this article in my report.
Thanks for your time,
Deidra Kalman

Subject: RE: ASCE Feedback (Contact us from www.asce.org)

Sent By "PERMISSIONS" <permissions@asce.org> On: April 5, 2010 5:38 AM

To: dkalman@ksu.edu

Dear Deidra Kalman:

Thank you for your permission request. Permission is granted to reuse Mechanical Properties of Steel Fiber-Reinforced Concrete tables and figures in your Master's Report.

Please add a full credit line to the material being reprinted: With permission from ASCE.

Xi Van Fleet

Senior Manager, Information Services

Publication Division

American Society of Civil Engineers

1801 Alexander Bell Drive

Reston, VA 20191

(703) 295-6278-FAX

PERMISSIONS@asce.org

Subject: Thank you for your Rightslink / Elsevier order

Sent By "Copyright Clearance Center" <rightslink@marketing.copyright.com> On: April 1, 2010 9:35 AM

To: dkalman@ksu.edu

Reply To: reply-fe531778716c017e711d-20206491_HTML-520825997-114453-6462@marketing.copyright.com

To view this email as a web page, go here.

To ensure that you continue to receive our emails,

please add rightslink@marketing.copyright.com to your address book.

RIGHTSLINK Copyright Clearance Center

COPYRIGHT CLEARANCE CENTER

Thank You For Your Order!

Dear Deidra,

Thank you for placing your order through Copyright Clearance Center's Rightslink service. Elsevier has partnered with Rightslink to license its content.

Your order details and publisher terms and conditions are available by clicking the link below:
http://s100.copyright.com/CustomerAdmin/PLF.jsp?ID=2010040_1270132532035

Order Details
Licensee: Deidra D Kalman
License Date: Apr 01, 2010
License Number: 2400250332035
Publication: Engineering Structures
Title: Blast testing of ultra-high performance fibre and FRP-retrofitted concrete slabs
Type Of Use: Thesis / Dissertation
Total: 0.00 USD

Please note: Credit cards are charged immediately after order confirmation; invoices are issued daily and are payable immediately upon receipt.

To ensure we are continuously improving our services, please take a moment to complete our customer satisfaction survey.

If you have any comments or questions, please contact Rightslink:
Toll Free: +1-877-622-5543
Tel: +1-978-646-2777
E-mail: customercare@copyright.com
Web: http://www.copyright.com B.1:v4.2

This email was sent to: **dkalman@ksu.edu**

Subject: Re: Copyright Permission

Sent By "Daniela Bedward" <Daniela.Bedward@concrete.org> On: March 31, 2010 1:20 PM

To: dkalman@k-state.edu

Attachments: Download all attachments

000907-1.png (86.2 KB, view as html, add to briefcase, download) 000906.png (2551.3 KB, view as html, add to briefc

Dear Deidra,

Please accept this e-mail as permission to reprint the requested figures detailed in the attached request form in your Master's report. Please be sure to credit ACI, the documents, and the authors.

Please feel free to contact me if you need further assistance.

Have a great day,

Daniela

Ms. Daniela A. Bedward
Publishing Services Assistant
American Concrete Institute
38800 Country Club Dr.
Farmington Hills, MI 48331 USA
Phone: (248) 848.3753
Fax: (248) 848.3701
E-mail: daniela.bedward@concrete.org
Website: www.concrete.org

Subject: RE: Permission for use of figures

Sent By "Dennis McCann" <dmccann@exponent.com> On: March 30, 2010 2:10 PM

To: dkalman@k-state.edu; sjsmith@ctlgroup.com

Deidra,

Thank you for asking. You are more than welcome to use the figure. Please just site the article in your report references.

Dennis

Dennis M. McCann, Ph.D., P.E.
Senior Managing Engineer
Exponent, Inc.
185 Hansen Court, Suite 100
Wood Dale, IL 60191
630-274-3206 office
630-730-8442 mobile
630-274-3299 fax
dmccann@exponent.com

-----Original Message-----
From: Deidra Kalman [mailto:dkalman@k-state.edu]
Sent: Tuesday, March 30, 2010 11:30 AM
To: Dennis McCann; sjsmith@ctlgroup.com
Subject: Permission for use of figures

Mr. McCann and Mr. Smith
I am a graduate student at Kansas State University and am doing my report on the use of steel fiber reinforced concrete in blast resistant design. I would like to ask your permission to use Figure 2 from your article, Blast Resistant Design of Reinforced Concrete Structures, in Structures Magazine April 2007 in my report. Please let me know what procedures you would like me to follow.

Thanks for your time,
Deidra Kalman